One way optical waveguides for matched non-reciprocal nanoantennas with dynamic beam scanning functionality

Yakir Hadad and Ben Z. Steinberg*

School of Electrical Engineering, Tel Aviv University, Ramat-Aviv, Tel-Aviv 69978, Israel
*steinber@eng.tau.ac.il

Abstract: Matching circuits for waveguide-nanoantenna connections are difficult to implement. However, if the waveguide permits only one-way propagation, the matching issue disappears since back-reflections cannot take place; the feed signal is converted to radiation at high efficiency. Hence, a terminated one-way waveguide may serve as an assembly consisting of a waveguide, a matching mechanism, and an antenna. Since one-way structures are inherently non-reciprocal, this antenna possesses different transmit and receive patterns. We test and demonstrate this concept on a recently suggested new class of one-way plasmonic waveguides and present an additional significant dynamic beam scanning functionality.

©2012 Optical Society of America

References and links

1. L. Novotny and N. V. Hulst, "Antennas for light," Nat. Photonics **5**(2), 83–90 (2011).
2. G. W. Hanson, "On the applicability of surface impedance integral equation for optical and near infrared copper dipole antennas," IEEE Trans. Antenn. Propag. **54**(12), 3677–3685 (2006).
3. L. Novotny, "Effective wavelength scaling for optical antennas," Phys. Rev. Lett. **98**(26), 266802 (2007).
4. A. Alu and N. Engheta, "Tuning the scattering response of optical nanoantennas with nanocircuit loads," Nat. Photonics **2**(5), 307–310 (2008).
5. A. Alù and N. Engheta, "Input impedance, nanocircuit loading, and radiation tuning of optical nanoantennas," Phys. Rev. Lett. **101**(4), 043901 (2008).
6. A. Alu and N. Engheta, "Herzian plasmonic nanodimmer as an efficient nanoantenna," Phys. Rev. B **78**(19), 195111 (2008).
7. M. Schnell, A. Garcia-Etxarri, A. J. Huber, K. Crozier, J. Aizpurua, and R. Hillenbrand, "Controlling the near-field oscillations of loaded plasmonic nanoantennas," Nat. Photonics **3**(5), 287–291 (2009).
8. T. Kosako, Y. Kadoya, and H. F. Hofmann, "Directional control of light by nano-optical Yagi-Uda antenna," Nat. Photonics **4**(5), 312–315 (2010).
9. X. Liu and A. Alu, "Subwavelength leaky-wave optical nanoantennas: directive radiation from linear arrays of plasmonic nanoparticles," Phys. Rev. B **82**(14), 144305 (2010).
10. D. V. Orden and V. Lomakin, "Fundamental electromagnetic properties of twisted periodic arrays," IEEE Trans. Antenn. Propag. **59**(8), 2824–2833 (2011).
11. A. G. Curto, G. Volpe, T. H. Taminiau, M. P. Kreuzer, R. Quidant, and N. F. van Hulst, "Unidirectional emission of a quantum dot coupled to a nanoantenna," Science **329**(5994), 930–933 (2010).
12. J. N. Farahani, D. W. Pohl, H. J. Eisler, and B. Hecht, "Single quantum dot coupled to a scanning optical antenna: a tunable superemitter," Phys. Rev. Lett. **95**(1), 017402 (2005).
13. A. F. Koenderink, "Plasmon nanoparticle array waveguides for single photon and single plasmon sources," Nano Lett. **9**(12), 4228–4233 (2009).
14. D. E. Chang, A. S. Sørensen, P. R. Hemmer, and M. D. Lukin, "Quantum optics with surface plasmons," Phys. Rev. Lett. **97**(5), 053002 (2006).
15. A. V. Akimov, A. Mukherjee, C. L. Yu, D. E. Chang, A. S. Zibrov, P. R. Hemmer, H. Park, and M. D. Lukin, "Generation of single optical plasmons in metallic nanowires coupled to quantum dots," Nat Lett. **450** 402–406 (2007).
16. Y. C. Jun, R. D. Kekatpure, J. S. White, and M. L. Brongersma, "Nanresonant enhancement of spontaneous emission in metal-dielectric-metal plasmon waveguide structures," Phys. Rev. B **78**(15), 153111 (2008).
17. T. J. Seok, A. Jamshidi, M. Kim, S. Dhuey, A. Lakhani, H. Choo, P. J. Schuck, S. Cabrini, A. M. Schwartzberg, J. Bokor, E. Yablonovitch, and M. C. Wu, "Radiation engineering of optical antennas for maximum field enhancement," Nano Lett. **11**(7), 2606–2610 (2011).

18. L. Yousefi and A. C. Foster, "Waveguide-fed optical hybrid plasmonic patch nano-antenna," Opt. Express **20**(16), 18326–18335 (2012).
19. A. Yaacobi, E. Timurdogan, and M. R. Watts, "Vertical emitting aperture nanoantennas," Opt. Lett. **37**(9), 1454–1456 (2012).
20. D. Dregely, R. Taubert, J. Dorfmüller, R. Vogelgesang, K. Kern, and H. Giessen, "3D optical Yagi-Uda nanoantenna array," Nat Commun **2**, 267 (2011).
21. Q. Song, S. Campione, O. Boyraz, and F. Capolino, "Silicon-based optical leaky wave antenna with narrow beam radiation," Opt. Express **19**(9), 8735–8749 (2011).
22. D. Ramaccia, F. Bilotti, A. Toscano, and A. Massaro, "Efficient and wideband horn nanoantenna," Opt. Lett. **36**(10), 1743–1745 (2011).
23. Y. Hadad and B. Z. Steinberg, "Magnetized spiral chains of plasmonic ellipsoids for one-way optical waveguides," Phys. Rev. Lett. **105**(23), 233904 (2010).
24. S. S. Walavalkar, A. P. Homyk, M. D. Henry, and A. Scherer, "Controllable deformation of silicon nanowires with strain up to 24%," J. Appl. Phys. **107**(12), 124314 (2010).
25. C. S. T. Studio, 2011 online: www.cst.com
26. L. Novotny and B. Hecht, *Principles of Nano-Optics* (Cambridge, 2006), Chap. 8.
27. Y. Xu, R. K. Lee, and A. Yariv, "Quantum analysis and the classical analysis of spontaneous emission in microcavity," Phys. Rev. A **61**(3), 033807 (2000).
28. B. Sepúlveda, J. B. González-Díaz, A. García-Martín, L. M. Lechuga, and G. Armelles, "Plasmon-induced magneto-optical activity in nanosized gold disks," Phys. Rev. Lett. **104**(14), 147401 (2010).
29. Y. Hadad and B. Z. Steinberg, "Green's function theory for infinite and semi-infinite particle chains," Phys. Rev. B **84**(12), 125402 (2011).
30. Z. Yu, G. Veronis, Z. Wang, and S. Fan, "One-way electromagnetic waveguide formed at the interface between a plasmonic metal under a static magnetic field and a photonic crystal," Phys. Rev. Lett. **100**(2), 023902 (2008).
31. H. Lira, Z. Yu, S. Fan, and M. Lipson, "Electrically driven nonreciprocity induced by interband photonic transition on a silicon chip," Phys. Rev. Lett. **109**(3), 033901 (2012).
32. Y. Mazor and B. Z. Steinberg, "Longitudinal chirality, enhanced nonreciprocity, and nanoscale planar one-way plasmonic guiding," Phys. Rev. B **86**(4), 045120 (2012).

1. Introduction

Antenna theory in the radio-frequency (RF) regime is a well-established discipline, whose overwhelming practical success can be attributed mainly to its conceptually modular nature. A RF signal is generated by an oscillator, and transferred by a waveguide to an antenna whose *remote* location is determined by system considerations. The waveguide is connected to the antenna via a feeding mechanism or matching circuit whose role is to eliminate back reflections if the waveguide and the antenna impedances mismatch. Directivity and gain are used to determine the radiated signal intensity, spatial properties and beam quality. Since most RF antennas are reciprocal, reciprocity theorem establishes symmetry between the antenna properties at transmit (Tx) and receive (Rx) modes.

An effort is devoted recently to the emerging field of nano-antennas designed to operate at optical or IR wavelengths. It is motivated by potential applications in diverse fields such as energy harvesting or concentration, local lighting/heating, sensing, wireless links, and more.

Despite the advancement in nano-scale technologies, a mere down-scale of RF antennas is not feasible due to fabrication limitations of e.g., matching-circuits and the profound change of metal properties when the frequency is increased to the optical regime [1]. Hence, the modular nature of RF antennas cannot be directly applied. New modeling and scaling tools of antenna elements that take into account material dispersion were developed [2,3] and applied for various classical as well as novel antenna geometries [1]. Other efforts are based on ad hoc tuning of classical geometries (e.g., nano-dipoles, Yagi-Uda antennas, nano-dimers) achieved by various antenna loading strategies, or geometrical tuning [4–8]. Leaky wave antennas based on particle chains were considered too, both in regular [9] and chiral [10] geometries. Some works match antennas to a nearby source [11–16], looking essentially at Tx operation. Alternatively, matching in Rx operation in the sense of maximizing received field intensities at the antenna's gap is addressed in [17]. However, the vibrant functionality so commonly available in RF systems, i.e., source to antenna energy transport via matched guiding remains largely unexplored; in most works the antenna radiates right from the source location in Tx mode, or matched right to its gap or another close point in Rx mode. An exception is the work in [18] where a patch nano-antenna is matched to a plasmonic waveguide by designing their impedances to be equal. In [19,20] antenna and antenna array are fed by waveguides, but the

matching is not studied directly, although in [20] it can be inferred indirectly through the ratio between the emission and the waveguide input (which is lower than the figures we report below). Finally, good matching is reported in [21,22], however the antennas in these works are of several microns wide.

Here we suggest a new concept for waveguide-nanoantenna assembly that, although not modular, encapsulates all the three important components in a matched and natural way. Thus it may offer a new kind of nanoantennas free from the difficulties discussed above. In our scheme, shown in Fig. 1, a terminated one-way plasmonic waveguide is the key component. Consider a guided mode that propagates, say, in the $+\hat{z}$ direction, in a conventional waveguide of finite length. Usually when it hits the termination most of its energy is reflected back into the waveguide. However, if it is a one-way waveguide these back reflections cannot take place so the guided mode is converted to radiation at high efficiency. This conversion takes place only in a limited region near the end that plays the role of a local antenna. Moreover, since one-way structures are inherently non-reciprocal, the antenna possesses *opposite* transmitting and receiving patterns, and a dynamic scanning functionality.

2. One-way guiding structure as a matched waveguide-antenna assembly

We use a recently suggested nano-scale one-way waveguide [23] as a demonstration platform. This waveguide is based on the interplay between two phenomena: the non-reciprocal optical Faraday (or cyclotron) rotation, and structural chirality. The former is obtained by exposing a sub-diffraction chain (SDC) of plasmonic particles to a longitudinal DC magnetic field $\mathbf{B}_0 = B_0\hat{z}$. The latter is obtained by constructing the SDC with non-spherical particles (for mathematical convenience, we choose prolate ellipsoids whose polarizabilty is known analytically) arranged as a spiral. The two-type rotations interplay enhances the non-reciprocity and leads to one-way guiding within a finite frequency band. The structure is shown in Fig. 1. Similar structures were fabricated in [24] for different applications. The system consists of N particles; the n-th is centered at $z_n = nd$, and rotated by $n\Delta\theta$ about the z axis. The chain is subject to an external magnetic field $\mathbf{B}_0$. Under the discrete dipole approximation, the chain response is governed by [23]

$$\boldsymbol{\alpha}_n^{-1}\mathbf{p}_n - \sum_{m\neq n}^{N}\mathbf{A}[(n-m)d]\mathbf{p}_m = \mathbf{E}^{inc}(\mathbf{r}_n) \qquad (1)$$

where $\boldsymbol{\alpha}_n$ and $\mathbf{p}_n$ are the n-th particle polarizability and dipole moment response, respectively. We have $\boldsymbol{\alpha}_n = \mathbf{T}_{-n}\boldsymbol{\alpha}\mathbf{T}_n$, where $\mathbf{T}_n$ is a transverse rotation matrix, $\boldsymbol{\alpha}$ is the polarizability of the reference ellipsoid subject to the longitudinal magnetic field $\mathbf{B}_0$, and $\mathbf{A}(z-z')\mathbf{p}$ is the electric field at z due to a short dipole $\mathbf{p}$ at z'. See [23] for details.

This formulation provides *initial parameter estimates*. The CST software [25] is used next to search for one-way/matched antenna operation parameters around the initial estimates, and to compute exact full-wave solutions with realistic material parameters.

In Tx the system is excited by a Quantum Emitter (QE) - a typical nano-scale light source. It is described by a spontaneous emission (SE) rate γ which can be divided into radiative and non-radiative parts, $\gamma = \gamma_r + \gamma_{nr}$, and for nanoantennas it is desired to maximize the quantum-yield $Q = \gamma_r/\gamma$ [26]. Due to modifications in its decay channels, the radiative part of γ may be enhanced comparing to the rate in vacuum γ_0. It can be achieved by placing the QE near a nanoantenna. This has been demonstrated experimentally and numerically [12–16]. Furthermore, the SE enhancement ratio is $\gamma/\gamma_0 = P_{in}/P_0$, where P_{in} is the extinct power on infinitesimal current dipole at the QE location $P_{in} = (1/2)\text{Re}\{\mathbf{E}\cdot\mathbf{J}^*\}$ and P_0 is the extinct power of the same dipole located in vacuum [26,27]. Therefore, in order to numerically model the

QE-antenna interaction and to estimate γ / γ_0 and Q we use a classical Short Dipole (SD) in the location of the QE as shown in Fig. 1, defining the *system port*.
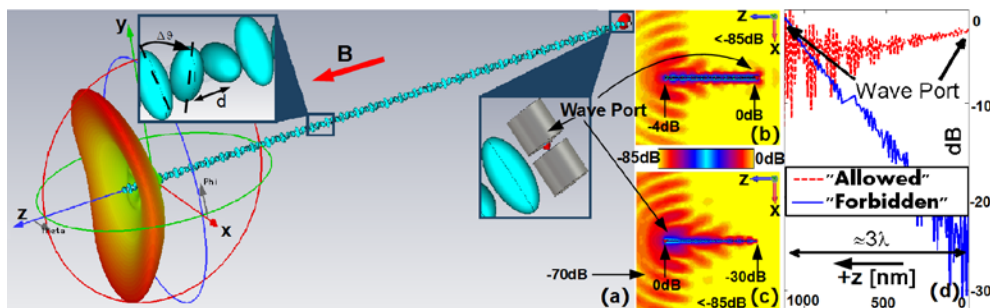

Fig. 1. The matched nanoantenna. (a) A general view with a typical far-field pattern. The chain is excited by a quantum emitter modeled as a short dipole, generating a guided mode that propagates in the (allowed) $+\hat{z}$ direction. Back reflections at the remote end cannot take place, hence the mode is converted to radiation. This end is a matched local antenna. (b) The near E-field. Energy is transmitted from the port to the remote end with minimal loss (4dB, due to material), and is emitted essentially from particles near the end. (Media 1 0.5Mb) (c) Due to the one-way property, if the port is located on the other end the chain excitation is marginal and the radiation is directly from the port. (d) Normalized fields at the center of each particle in Figs. 1(b-c). Dashed [solid] lines– corresponds to Fig. 1(b) [1(c)], source at $z = 0$ ($z = 103d$).

We discuss now traditional parameters used to characterize antenna performance, and relate them to the quantities above. A classical measure of the feeding quality, i.e. the matching between the system port and the antenna radiating elements (in the other end of chain), is Γ_{11} - the reflection coefficient. It is defined as the ratio between the chain modes that propagate in the $+\hat{z}$ and $-\hat{z}$ directions. It can be obtained by applying a discrete Fourier transform (DFT) on the chain dipole moments $\mathbf{p}_n^r = \mathbf{T}_n \mathbf{p}_n$ near the port region and computing the ratio between the spectral components that correspond to $-\hat{z}$ and $+\hat{z}$ propagations ($\mathbf{T}_n$ is present to eliminate spurious side-lobes at $\pm \Delta \theta$ due to the structure rotation). Low Γ_{11} indicates good matching, but may also indicate that much of the energy injected to the chain is absorbed by loss. Hence, one may look at the transmission coefficient Γ_{12}: the ratio between the $+\hat{z}$ propagating waves near the chain end and near the port. For our case, a good antenna system is characterized by $| \Gamma_{11} | \ll 1$ and $| \Gamma_{12} | \approx 1$.

In Tx mode, the antenna gain in the direction $\hat{r}$, $G_T(\hat{r})$, is

$$G_T(\hat{r}) = S^{FF}(\hat{r}) / \max_{\theta,\phi} S_{sdFS}^{FF}(\hat{r}), \quad \text{with} \quad \oint G_T d\Omega = 4\pi \gamma_r / \gamma_0 \qquad (2)$$

where $S^{FF}(\hat{r})$ and $S_{sdFS}^{FF}(\hat{r})$ are the far-field Poynting vector radiated by our antenna and by our SD port in free space respectively, both with the same current. Assuming that in free space the QE is approximately isotropic – the second equality in Eq. (2) is valid. Hence, the gain includes also a measure of the matching between the QE and our antenna assembly. Finally, the antenna *radiation efficiency* is given by

$$\mathcal{E} = P_{FF} / (P_{FF} + P_{Abs}) = \gamma_r / \gamma = Q \qquad (3)$$

where P_{FF}, P_{Abs} are the power that gets to the far field, and the power absorbed by the antenna material loss, respectively. In Rx the system is excited by an incident plane wave that illuminates the entire assembly - the optical signal that the antenna should receive. The current excited in the system port $\mathbf{J}$ is the "received signal". The antenna gain is then given by

$$G_R(\hat{r}) = |\mathbf{J}|^2 / |\mathbf{J}_{sdFS}|^2 \tag{4}$$

with $\mathbf{J}_{sdFS}$ - the response of identical SD under the same incident field - *located in free space*.

3. Numerical study and conclusions

We turn now to demonstrate the antenna operation of this structure, using the entities defined above. We concentrate in the one-way lower band [23]. The chain consists of 103 ellipsoidal particles with semi-axis $a_x = 10\,\text{nm}$, $a_y = a_z = a_x / 2$ and $d = 11\,\text{nm}$. The rotation step is $\Delta\theta = 60°$. Material parameters correspond to Ag, with $\omega_p = 2\pi 2150\,\text{THz}$, and loss rate of $\tau^{-1} = 4.3\,\text{THz}$ [9]. A 20 nm dipole emulates the QE (see Fig. 1(a)). The magnetic field corresponds to $-q_e B_0 / m_e \equiv \omega_b = 0.04 - 0.05\omega_p$. Due to the particles quasistatic plasmonic resonance, the magnetic response remains significant despite losses [28]. With these parameters, one-way guiding in the $+\hat{z}$ direction is created at a finite bandwidth of about 29 THz around the frequency $f = 780 - 790\,\text{THz}$. We have excited the chain in the Tx mode and solved for the chain response using CST [25]. Typical responses that show the one-way property and near fields at 791 THz with $\omega_b / \omega_p = 0.04$ are shown in Fig. 1(b)-1(d) (Media 1).

Figure 2(a) shows the spatial DFT of $\mathbf{p}_n^r$ over 25 particles near the port. Negative (positive) βd corresponds to propagation in the positive (negative) z-direction. When $B_0 = 0$ ($\omega_b = 0$, one-way is turned off) the spectrum peaks indicate guided mode to guided mode strong back reflection, and material loss of about $-7.7\,\text{dB}$ per roundtrip. The peak locations are symmetrical around the origin, and correspond to the guided mode roots of the chain determinant [23] when no magnetic field is present. When $\omega_b = 0.05\omega_p$ (one way turned on), the peaks shift to non-symmetrical locations. The left (right) peak correspond exactly to the root of the one-way chain determinant [23], representing $+\hat{z}$ ($-\hat{z}$) propagating guided (radiation) mode (the group and phase velocities are in opposite signs [23]). The back reflection peak is reduced considerably since the back reflected mode is a radiation mode that loses its energy very fast; it radiates to the free space. Γ_{11}, given as the ratio between the backward and forward peaks, is shown in Fig. 2(b). The antenna is well matched over the entire one-way regime. The transmission coefficient Γ_{12} that measures the material loss along the chain is computed similarly by using the ratio between the peaks at negative βd in the DFT near the port and near the remote end. Note that it is nearly flat about $-4\,\text{dB}$, consistent with the loss estimated from Fig. 1(b) and from the $\omega_b = 0$ curve in Fig. 2(a).

Figure 2(c) shows the radiation efficiency $\mathcal{E}$ given in Eq. (3) for the entire assembly including the unavoidable insertion loss of the waveguide. More specifically, $\mathcal{E}$ is calculated in 3 steps. First, the total far-field power is calculated by surface integrating pointing's vector on the solution's air-box boundary. The absorbed power in the structure is calculated by volume integration of $\text{Re}\{\mathbf{E}\cdot\mathbf{J}^*\}$. Summing up these two, we obtain the total power provided by the lumped source. Finally, the radiation efficiency is obtained by (Radiated power)/(Total injected power). Note that although the total efficiency of the system is about $-4.4\,\text{dB}$ (37%), the matching plus antenna efficiency is quite *high and flat* $-4.4-(-3.5) = -0.9\,\text{dB}$ (81%) in the *entire one-way band*. It should be emphasized that the $-3.5\,\text{dB}$ component is only due to propagation in the waveguide and is in principle inherent to any waveguide-fed antenna. The antenna gain in both Tx and Rx modes are shown in Fig. 3(a) with the one-way property, and in Fig. 3(b) without it. In the former the gain and beam quality are high, and in the latter they reduce considerably. Additional interesting observations can be made. Since the structure is non-reciprocal, the Tx and Rx gain curves in Fig. 3(a) point at opposite directions; the antenna transmits at angle θ_T, and receives from $\theta_R = 180° - \theta_T$. This is a result of the longitudinal

phase-matching required between the chain modes and the free-space waves in Tx and Rx, and the asymmetric spectrum of the structure (corresponding to the asymmetric locations of the roots of the one-way chain determinant [23]). If the one-way property is turned off, the system becomes reciprocal hence Rx and Tx gain curves are identical as seen in Fig. 3(b).
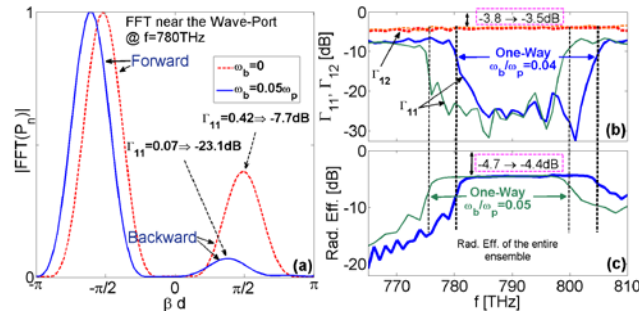

Fig. 2. Antenna matching in Tx. (a) A DFT of the chain response. (b) reflection (transmission) coefficient - solid lines (dashed lines) vs. frequency for two levels of magnetization. (c) Radiation efficiency of the entire structure.

With the present parameters, chain length is $\approx 3\lambda$; the observed multi-lobe low gain is typical to long wire radiation and is due to the chain length and the fact that for conventional (two-way) chain the reflection magnitude at the chain terminations is nearly a unity [29]. The fact that with the one-way property the beam is collimated and possesses high gain is due to the near perfect matching and due to the coherent radiation mode from the vicinity of the chain end. This is seen in E-field plot of Fig. 1(b) (Media 1). Essentially, only a section of ≈ 30 particles ($\approx 1\lambda$) at the chain end radiates to the free space, and can be considered as a "local antenna". As a direct result, we have observed that the gain does not change when the chain length is increased. Finally we note that the bias magnetic field can be varied widely without deteriorating the one-way property, but with considerable change of the radiation mode complex wave-number. Hence, our system possesses a dynamic beam scanning. A change of B_0 by $\pm 20\%$ causes a $60°$ variation of Tx and Rx directions, as shown in Fig. 4.
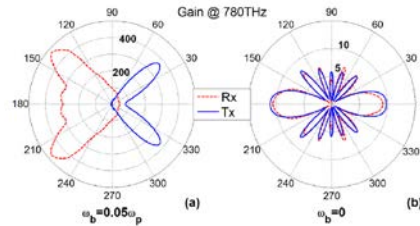

Fig. 3. Antenna Tx and Rx gain in the plane. (a) One way is on. (b) One way is off. The beam is conical; hence gain in plane is the same.
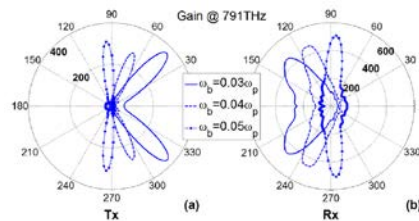

Fig. 4. Dynamic control of the optical beam by the bias magnetic field. (a) Tx gain. (b) Rx gain.

We conclude our discussion by commenting that the concepts presented here may be applied to any one-way guiding scheme, e.g., [30–32] leading to potentially perfect matching of nanoantennas to feeding and guiding systems.